HiSST: 2nd International Conference on
High-Speed Vehicle Science Technology
11–15 September 2022, Bruges, Belgium

Table-Top Shock Tunnel (TTST) for Studies of Shock Layer Chemistry and Rapid and Low-Cost Testing of Materials for Hypersonics

Brian E. Riggs,[1] Eric C. Geistfeld,[2] Chenbiao Xu,[1] Irina Gouzman,[1] Thomas E. Schwartzentruber,[2] Timothy K. Minton*[1]*

Abstract

A new "table-top shock tunnel (TTST)" has been constructed and is intended to allow rapid and low-cost measurements of shock-layer chemistry and material response in well-characterized high-velocity flows. The TTST is based on the production of pulsed hypersonic molecular beams by laser detonation in a conical nozzle. In addition to providing fundamental data for the development of models, the production of controlled shock layers above ablating and non-ablating surfaces and the measurement of their phenomenology provide a means to validate new models. Furthermore, material response can be tested in realistic environments and aid in the development of materials for hypersonics applications. Initial characterization of the TTST has been carried out by studying the ablation phenomenology of a Kapton H polyimide surface exposed to a hypersonic O/O_2 beam at various distances from the nozzle throat and comparing the experimental observations with the results of DSMC calculations.

Keywords: *Molecular beam, atomic oxygen, Kapton ablation, shock tunnel, DSMC*

Nomenclature

TPS – Thermal Protection System
CARS – Coherent AntiStokes Raman Spectroscopy
REMPI – Resonance Enhanced Multiphoton Ionization
LIF – Laser Induced Fluorescence
TEA – Transversely Excited Atmospheric
SEM – Scanning Electron Microscopy
AFM – Atomic Force Microscopy
DSMC – Direct Simulation Monte Carlo

1. Introduction

Hypersonic ablation of a thermal protection system (TPS) material in air involves four coupled flow regimes [1], as depicted in Fig. 1. These include (1) shock-induced dissociation of air molecules, (2) air chemistry involving gaseous ablation products (e.g., CO and CO_2 for a carbon-based TPSs), (3) diffusion of reactive species to the TPS surface, and (4) local gas-surface chemical reactions. Current experimental measurements of the shock and boundary layers (subsequently referred to collectively as the "shock layer" in this paper) are difficult and expensive to perform, and ground-based experiments simply cannot reproduce the wide range of potential flight conditions. Therefore, accurate predictive models are required for use in computational fluid dynamics simulations. The most widely used vibrational energy model is the Millikan-White model [2], and the most widely used dissociation model

[1] *Dept. of Aerospace Engineering Sciences, University of Colorado, Boulder, CO 80303-0429 United States, tminton@colorado.edu*
[2] *Dept. of Aerospace Engineering and Mechanics, University of Minnesota, Minneapolis, MN 55455 United States, schwart@umn.edu*

is the Park TTv model [3]. Both these models are empirical and based on relatively few experimental data sets. Their accuracy outside of the limited experimental conditions is uncertain, and this uncertainty directly affects the prediction of all other coupled processes shown in Fig. 1.

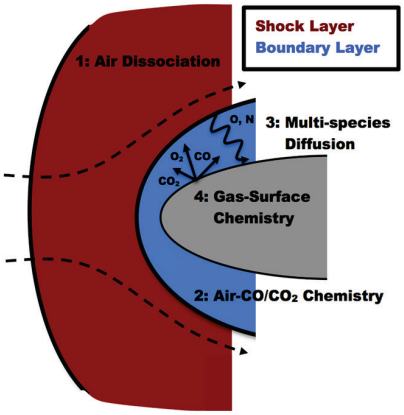

Fig 1. Flow regimes relevant to hypersonic ablation. (Not to scale.)

To reduce this uncertainty, a significant amount of research has been performed using computational chemistry [4-9]. These first-principles, predictive simulations and models have been shown to reproduce the limited experimental results [2,10-12] used to construct the empirical Millikan-White and Park TTv models. However, the first-principles calculations differ significantly from these empirical models for other hypersonic conditions where no experimental data exist [6,7,9]. For this reason, new optical diagnostic data measured under relevant hypersonic flow conditions are needed to validate these new models. Such experiments are extremely challenging and expensive, and no such data sets, sufficient to validate new models, have been generated to date.

A key challenge of testing in ground-based facilities is that true hypersonic conditions can only be sustained for short test times (microseconds to milliseconds). Collecting optical diagnostic data, for example, during such short timescales in a high-temperature gas is extremely difficult (low signal to noise). Furthermore, high-enthalpy facilities tend to be large facilities where only a few tests can be performed per day and precise repeatability between tests is difficult. Examples of such facilities are located at CUBRC [13], the University of Queensland [14], NASA Ames (EAST facility) [15], and Stanford University [12]. Alternatively, lower-enthalpy facilities have longer test times, and therefore optical measurements can be made more easily. However, the relevant thermochemical nonequilibrium processes in the shock layer are no longer present. Such facilities include those at the University of Canberra [16], Caltech (formerly located at the University of Illinois) [17], and Ohio State University [18].

We have attempted to fill a gap in hypersonic testing with the development of a new apparatus for investigating shock layer physics under relevant conditions. The basic idea is that a high-velocity pulsed molecular beam, when targeted at a small blunt object, can generate a hypersonic shock layer that exhibits relevant dissociation physics and ablation chemistry. Unlike large shock-tunnel facilities, the free stream is well characterized, and the beam (and therefore the shock layer) can be generated (pulsed) 2-3 times per second for hours or even days with repeatable conditions, providing a practical laboratory environment for detailed investigations of shock layer chemistry and physics, as well as ablation phenomena. Despite its relatively small size, the new instrument can be used for rapid acquisition of high-fidelity data on shock layer chemistry that will provide definitive validation of emerging models. This facility fits in a common laboratory space, and the vacuum chamber (including the hypersonic beam, target, and beam diagnostics) occupy a footprint smaller than a typical laser table. Thus, **this instrument is referred to as a "Table-Top Shock Tunnel" or "TTST"**. The hypersonic beam is based on the laser-detonation source [19-23] that has been used in studies of hyperthermal gas-phase and gas-surface scattering dynamics, mainly related to atomic-oxygen effects on materials in low Earth orbit. This beam can create reproducible and intense pulses of gas with nominal velocities of 6-9 km s^{-1} at repetition rates of 2-3 Hz.

The transformative novelty of the TTST is threefold. (1) A well characterized gas or gas mixture (in terms of velocity distribution, mole ratio, and chemical state) can be directed at a target. (2) The high

repetition rate and reproducibility of hypersonic pulses of sufficient intensity to form a shock above a target allows for high quality spectroscopic data to be obtained with standard diagnostic tools, such as optical emission, coherent anti-Stokes Raman spectroscopy (CARS) or, possibly, laser induced fluorescence (LIF). (3) The target may be ablating or non-ablating; in the case of an ablating material, the sample may be heated to high temperatures, allowing for the investigation of the boundary layer above an ablating material as well as studies of the ablated surface. This experimental setup is not appropriate to study fluid dynamic phenomena such as high Reynolds number flow (transition and turbulence), shock-boundary layer interactions, separated flow, and it cannot exactly reproduce free-stream flight conditions. Nevertheless, no ground-based facility can capture all flight-relevant processes and provide a feasible means for optical measurements. The TTST concept focuses specifically on producing data for nonequilibrium dissociation, vibrational and rotational populations, and gas-surface interactions. It is this focus that may enable the TTST to obtain high-quality fundamental data for relevant conditions that no other existing facility can.

2. Experimental Details

A diagram of the TTST facility is shown in Fig. 2. The heart of the TTST is a laser-detonation hypersonic beam source [19-23]. A pulsed valve is used to inject gas at high pressure (>550 psi) into the 1 mm diameter throat of a conical nozzle. After the gas expands into the nozzle, a 7-12 Joule per pulse CO_2 TEA laser is fired, and the light is focused down into the nozzle where it induces a breakdown and heats the resulting plasma to 40,000 – 50,000 K in the confined space near the nozzle throat. The detonation wave that is produced dissociates and accelerates the gas, and a neutral pulse emerges from the nozzle, containing partially dissociated gas, with the extent of dissociation depending on various operating parameters of the source. The pulse has a velocity distribution of ~2000 m s^{-1} full width at half maximum (fwhm), and the nominal velocity can be varied from about 6 to 9 km s^{-1}. Beams may be produced with precursor gases, O_2, N_2, Ar, CO_2, and N_2O. Mixtures of these gases may also be used, and one can imagine additional precursor gases. For diatomic and polyatomic precursor gases, there is considerable dissociation in the nozzle. The repetition rate of the source is currently limited to 2-3 Hz by pumping constraints. The hypersonic beam source is attached to a main "shock chamber," where a target object may be placed. The base pressure of this chamber is ~10^{-7} Torr. Optical beams for future Schlieren and laser-based diagnostics will pass through the main shock chamber. The position of the object is variable, with nozzle-throat-to-sample distances of 15-65 cm. The allowable sample area increases with distance, but a sample diameter of 25 mm is possible at all distances. The pulse width

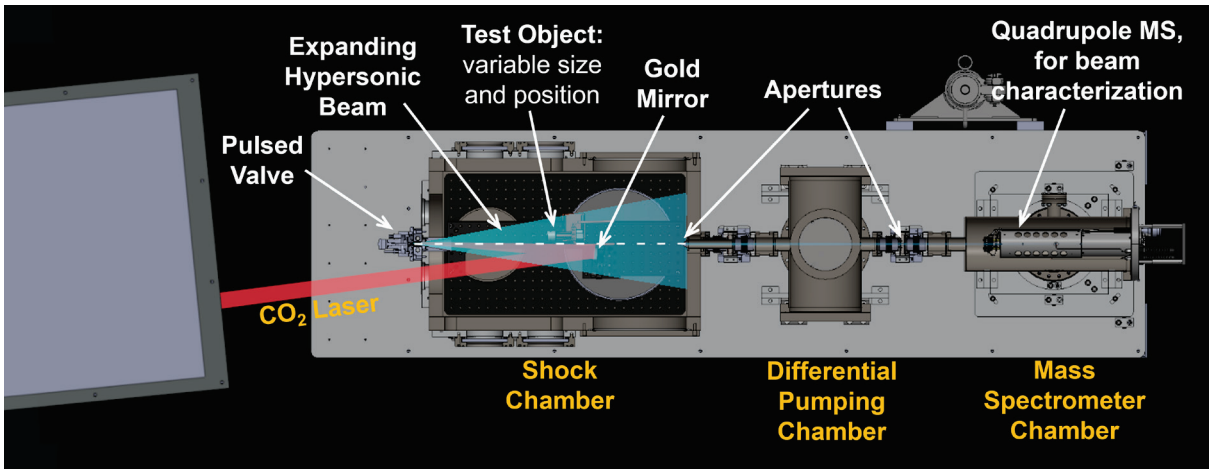

Fig 2. Diagram of the table-top-shock tunnel (TTST).

of the beam is determined under the assumption of a point source at the nozzle throat, with the distance to the object and velocity distribution of the beam yielding a minimum pulse width (fwhm) of ~20 μs. The mole fractions of the species in the hypersonic beam and their velocity distributions are characterized using the time-of-flight method by a differentially pumped mass spectrometer (base pressure ~10^{-9} Torr). Based on earlier studies, we assume that O and O_2 produced from the source operating with pure oxygen as the precursor gas are in their ground electronic states, $O(^3P)$ [24] and

$O_2(^3\Sigma_g^-)$ [25]. Unpublished results also suggest that N atoms produced with N_2 as the precursor gas are in their ground $N(^4S)$ state. Example characteristics of two beams that have been produced from either pure oxygen or nitrogen precursor gases are a shown in Fig. 3. If desired in the future, the differentially pumped region (base pressure ~10^{-8} Torr) could be used for additional characterization of the internal state distributions of the species in the beam, for example, by resonance enhanced multiphoton ionization (REMPI). CARS could be used in main chamber to measure the vibrational populations of molecular species, such as O_2 and N_2, in the beam (with the object removed). The entire length of the basic vacuum chamber portion of the instrument is ~2 m, and the lasers and detection equipment may be placed around this chamber. Thus, the entire facility is housed in the space of a typical university laboratory.

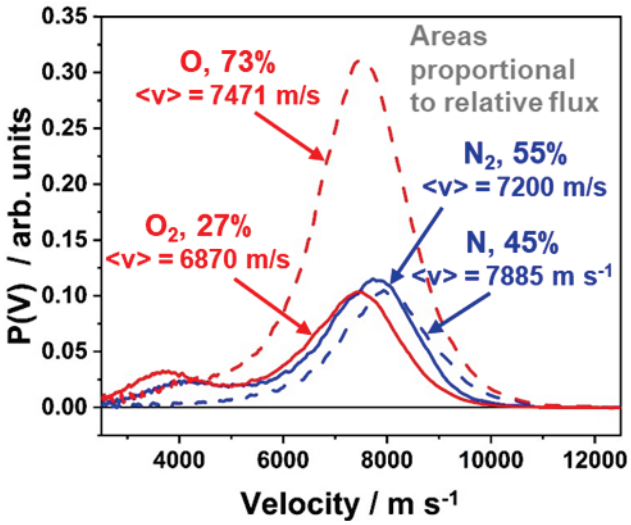

Fig 3. Velocity distributions of components of two hypersonic molecular beams. Red curves show the velocity distributions of the O and O_2 components of a beam formed from pure O_2 as the precursor gas. Blue curves show the velocity distributions of the N and N_2 components of a beam formed from pure N_2 as the precursor gas. Mole fractions of the atomic and molecular components of each beam are also shown.

3. Results and Discussion

Initial characterization of the TTST has been conducted by exposing Kapton H polyimide samples (125 μm thick) to a hypersonic O-atom beam, whose characteristics are shown by the red curves in Fig. 3. The choice to expose Kapton H for the initial study was based on the extensive knowledge of the effects of atomic oxygen on Kapton H, both in the low Earth orbital environment [26] and in hyperthermal O-atom beams in the laboratory [27]. In a highly rarefied flow of O atoms with ~7.8 km s^{-1} velocity, the erosion yield of Kapton H is known to be 3.0×10^{-24} cm^3 $O\text{-}atom^{-1}$. Therefore, by measuring the mass loss of Kapton H samples, with a known density of 1.42 g cm^3, at a distance from the nozzle throat where the O atoms in the beam are largely unimpeded by gas-phase scattering above the surface (i.e., where gas compression above the sample is negligible), then the flux of the hypersonic beam may be determined. The beam flux at other distances from the nozzle throat may then be determined from the assumption of a $1/r^2$ dependence. Besides allowing for the determination of the beam flux, the use of Kapton H provides insight into the formation of a shock above the sample surface through the examination of the surface morphology that develops as the surface is etched, as will be seen below.

Kapton H samples of 19 mm diameter were placed in a mount with an overall diameter of 25 mm. Samples were typically exposed to the beam at a variety of distances from the nozzle throat, from 20 cm to 65 cm, for 50,000 pulses of the hypersonic beam source, operating at a repetition rate of 2 Hz. The sample surfaces were oriented perpendicular to the streamlines of the flow at the sample centre. In addition, the exposed samples were examined by scanning electron microscopy (SEM) and atomic force microscopy (AFM). In some cases, longer exposure durations were used. The masses of the

samples were found by weighing them before and after exposure (with appropriate desiccation prior to each measurement).

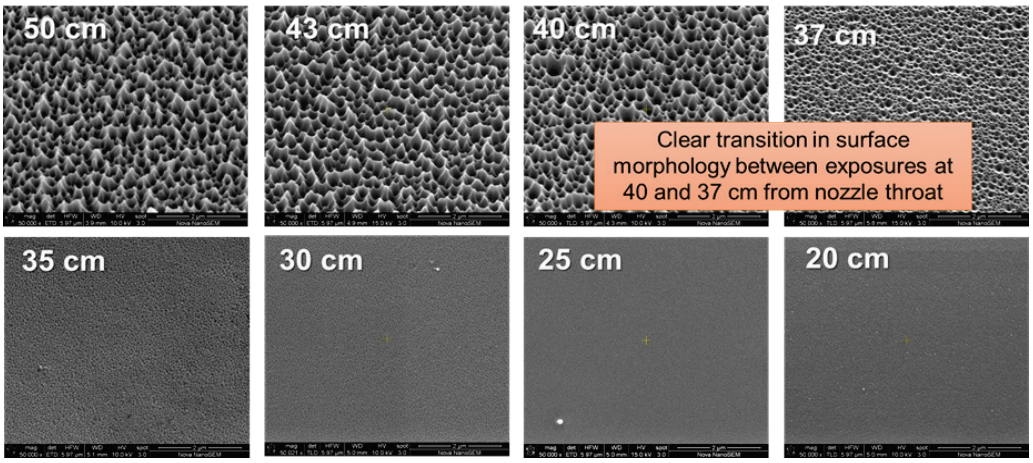

Fig 4. SEM images of Kapton H surfaces that were exposed at various distances (as indicated) from the throat of the hypersonic nozzle. All SEM images were collected from the centre of the exposed sample with a magnification of x20,000.

As seen in Fig. 4, the surfaces that were etched at 40, 45, and 50 cm from the nozzle throat became very rough, similar (though not identical) to Kapton H surfaces than have been exposed to atomic oxygen in low Earth orbit [28], where the flow onto the surface may be assumed to be free molecular. There is an abrupt change in surface roughness, from rough to smooth, as the sample is brought closer to the nozzle, indicating that the development of the surface texture is very sensitive to the exact gas-surface conditions. The disappearance of surface texture is attributed to the increasingly broad angle of attack from impinging O atoms, which is expected when incident O atoms encounter a higher density of gas above the sample, resulting from the increasing O/O_2 flux with decreasing nozzle-sample distance.

Near the transition region, where the surface roughness is changing rapidly with nozzle-sample distance, the surface roughness varies dramatically from the centre of the sample to the outer edge. Fig. 5 shows a series of atomic force microscope (AFM) images from smaller to larger radii from the centre of a single sample exposed at 37 cm from the nozzle throat. The transition to a smoother surface texture at this distance (Fig. 4) suggests that the etching of the Kapton H surface is no longer governed mainly by O atoms that strike the surface unimpeded. Thus, the nozzle-throat-to-sample distance of 37 cm may correspond the formation of a weak shock above the surface. Quantitative examination of the surface roughness from the sample that was exposed at this distance shows that the surface roughness

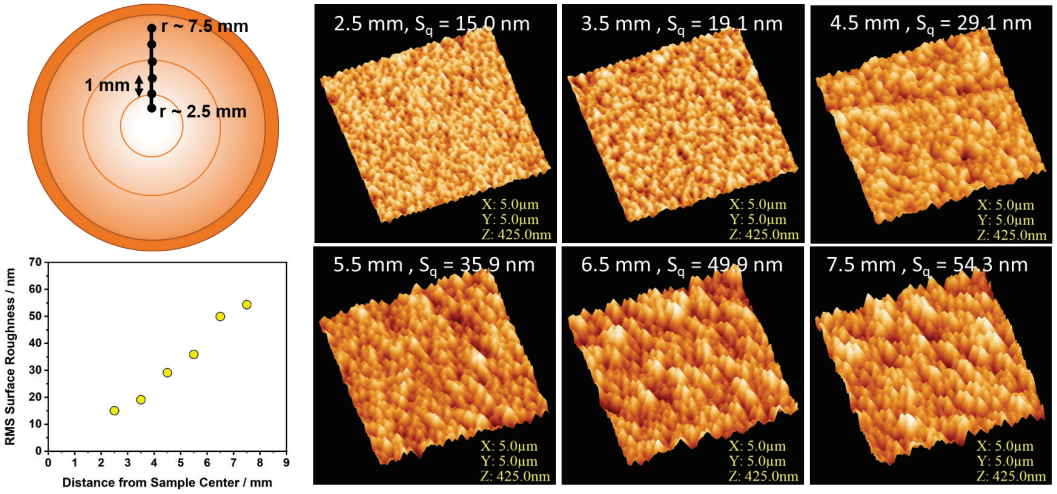

Fig 5. AFM images of Kapton H sample exposed to the hypersonic O/O_2 beam at 37 cm from the nozzle throat as a function of distance from the centre of the sample. The lower-left graph shows that the root mean square (rms) roughness changes by a factor of ~4 over the range of radii studied.

increased dramatically from the centre to the edge. This observation is consistent with the supposition that a weak shock layer is causing gas-phase collisions to randomize the angles at which the incoming, high-velocity O atoms strike the surface and lead to a smoother surface texture. It is expected that the gas compression would be stronger at the centre than the edges of the sample.

Direct simulation Monte Carlo (DSMC) calculations were performed to investigate the relationship between the gas-dynamic conditions above the samples and the observed roughness. We have used the Molecular Gas Dynamics Simulator implementation of the DSMC method developed at the University of Minnesota [29]. The simulation conditions are shown in Table 1 and the simulation domain is pictured in Fig. 6. We have used the Variable Hard Sphere model for collisional cross sections, a constant collision number for rotational relaxation, and Millikan and White vibrational relaxation times.

Table 1. DSMC simulation conditions for this study.

#	Representative Distance / Condition	Freestream O Atom Flux (Molecules m^{-2} s^{-1})	Composition	ρ_∞ (kg m^{-3})	Velocity Sampling
1	20 cm	4.76×10^{25}	$\chi_O = 0.724$ $\chi_{O_2} = 0.256$	4.91×10^{-5}	V_X: Beam Distributions V_Y and V_Z : Boltzmann @ 10 K
2	25 cm	1.19×10^{25}		3.14×10^{-5}	
3	30 cm	4.64×10^{24}		2.18×10^{-5}	
4	35 cm	2.61×10^{24}		1.60×10^{-5}	
5	40 cm	2.00×10^{24}		1.23×10^{-5}	
6	45 cm	1.58×10^{24}		9.70×10^{-6}	
7	50 cm	1.01×10^{24}		7.86×10^{-6}	
8	65 cm	7.57×10^{23}		4.65×10^{-6}	
9	Low Earth Orbit	1.5×10^{19}	$\chi_O = 0.909$ $\chi_{N_2} = 0.091$	5.85×10^{-11}	(7500,0,0) m/s With 3D Boltzmann @ 1000 K

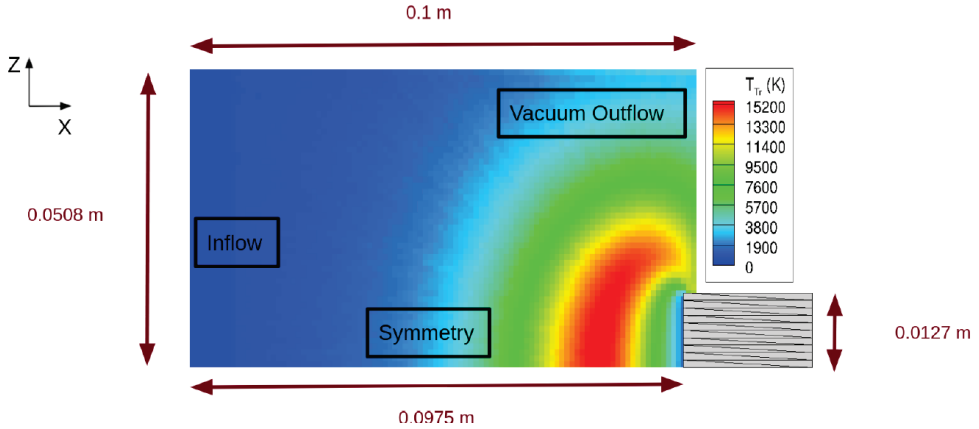

Fig 6. DSMC simulation domain.

The inflow conditions were kept constant in time, and each simulation was run until it reached steady state, then results were sampled. Inflow flux was varied using the $1/r^2$ flux-distance relation in ratios corresponding to nozzle-sample distances of 20, 25, 30, 35, 40, 45, and 50 cm based on an estimate of the flux at 40 cm, obtained from the mass loss measurements of Kapton H at this distance. The estimated peak flux of O atoms at 40 cm from the nozzle throat was determined to be 2.0×10^{24} O atoms m^{-2} s^{-1} during the ~20 μs beam pulse. It was further determined that, during this short period, the compression above the sample quickly reached a steady state, so the DSMC calculations assumed a constant flux at the peak-flux value. The velocity distributions sampled for the x component of the velocity (V_x, perpendicular to the sample surface) were the measured O and O_2 distributions shown in Fig. 3. The V_y and V_z sampling distributions were assumed to be Maxwellian at 10 K. Rotational and vibrational energies of O_2 were sampled from Boltzmann distributions at 2500 K. The mole fractions of the O and O_2 in the inflow were taken as the measured values (Fig. 3). The modelled diameter of the object corresponded to the actual diameter of the sample + holder (i.e., 25 mm). All atoms and

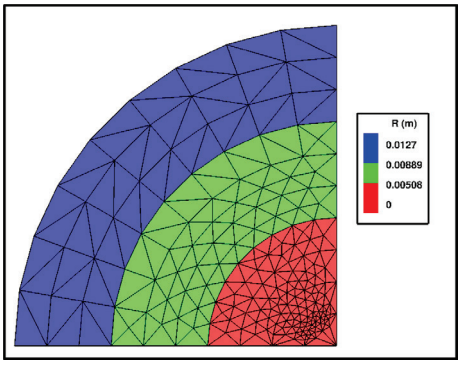

Fig 7. Target face split into three radial regions, labeled Center, Mid, and Edge in results.

molecules that struck the surface were assumed to desorb in thermal equilibrium at 22 °C, the sample temperature in the experiment. Characteristics of particles that impacted the surface were stored and plotted in distributions. The surface was split into three regions to characterize the changing surface flux at different radial stations, called Center, Mid, and Edge (see Fig. 7). An example of the simulated temperature profile of the flow over the test object at 25 cm from the nozzle throat is shown in Fig. 8.

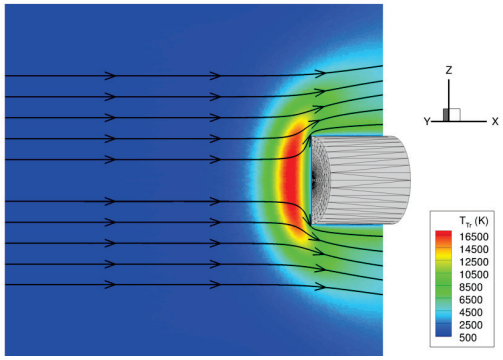

Fig. 8. DSMC simulation of the temperature of the flow over the 25 mm diameter object at 40 cm from the nozzle throat.

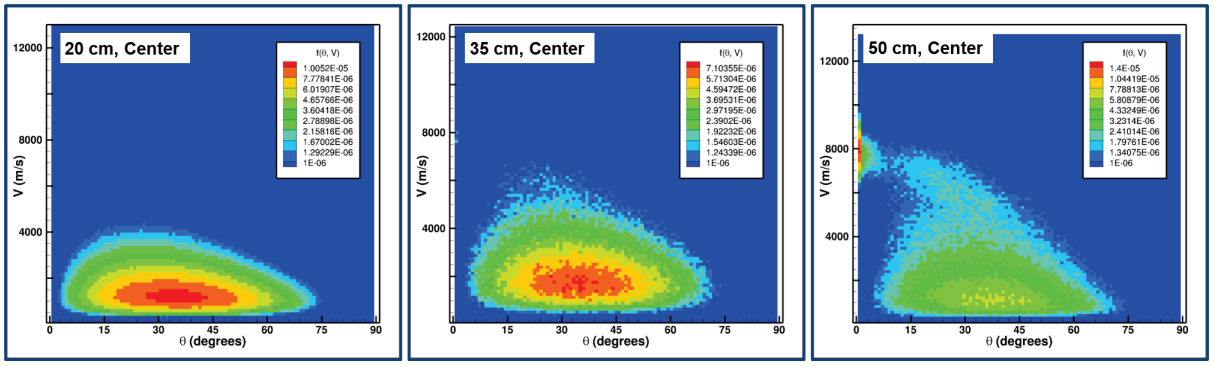

Fig. 9. DSMC results showing the relationship between O-atom velocity and impingement angle onto the surface (with respect to the surface normal) for the Centers of samples exposed at 20, 35, and 50 cm from the nozzle throat.

Fig. 9 shows flux maps of O atoms that strike the centres of sample surfaces that were exposed at 20, 35, and 50 cm from the nozzle throat, as a function of velocity and impingement angle. Clearly, as the inflow density is lowered (i.e., increasing distance), the distributions have more of their flux at low angles and high velocities, implying that, as the distance is increased, the shock formed in the beamline becomes increasingly diffuse, and incoming O-atoms are less likely to undergo gas phase collisions before they impact the surface. The significant fraction of unimpeded O atoms is strongly correlated

with the development of surface roughness, although the interplay between the effects of primary vs. secondary O-atom collisions on the surface texture is unknown at this time.

The nozzle-sample distance that showed the largest change in the flux of unimpeded O atoms (V ~ 8000 m s^{-1}) across the surface was 35 cm (see Fig. 10), which is very close to the distance (37 cm) where the largest difference in surface roughness was seen across the sample (see Fig. 4). The large difference between unimpeded particles across the surface is expected when the compression is such that the pressure at the stagnation point is sufficient to deflect most incoming atoms and molecules while the pressure near the outer edge of the sample is low enough to allow many O atoms to strike the surface unimpeded. The correlation between the calculated change in unimpeded O atoms and the rapid change in surface roughness is remarkable and suggests that the DSMC results capture the essential flow dynamics. These results predict that, under these initial experimental conditions, the density at the stagnation region for the sample at 20 cm from the nozzle is approximately 4×10^{-3} kg m^{-3}, corresponding to a pressure of ~4 Torr. Higher compression may be possible if the object is moved closer to the nozzle or if the nozzle throat diameter is increased allowing more gas to be processed by the laser, which has adequate pulse energy to produce beams with similar velocity and O/O_2 mole fractions having at least 1.5x higher flux. Higher fluxes may also be achieved by producing beams with lower velocities, for example, 6000 - 7000 m s^{-1}. With lower velocity and thus lower translational energy per particle, more gas can be processed with a given laser pulse energy.

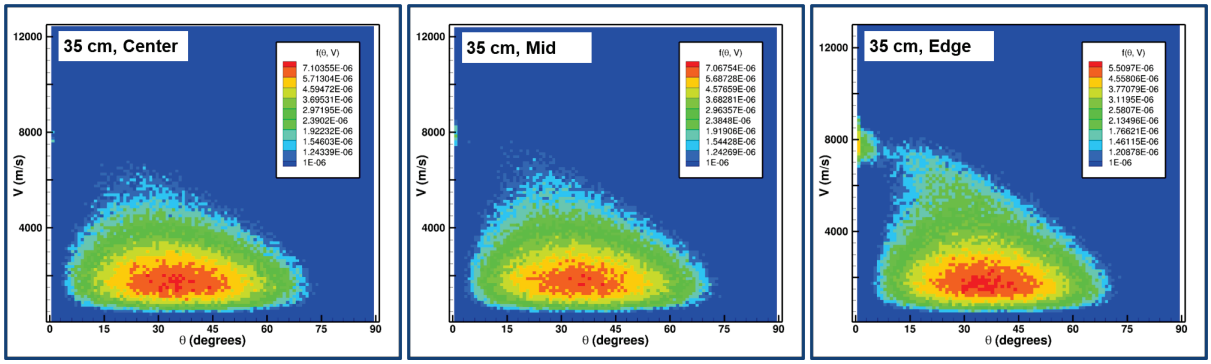

Fig 10. DSMC results showing the relationship between particle velocity and impingement angle onto the surface (with respect to the surface normal) for a sample at 35 cm from the nozzle throat, at the sample Center, Mid, and Edge.

4. Conclusion

Current hypersonic ablation models are empirical and are unable to predict conditions in a hypersonic shock layer, and new models under development are limited by the paucity of high-quality data needed for their refinement and validation. A new approach, referred to as a table-top shock tunnel (TTST) has been developed for measuring shock layer chemistry and conducting rapid and low-cost materials testing under relevant hypersonic conditions. The approach is to use existing laser-detonation technology, optimized for high flux operation, to produce a hypersonic pulsed molecular beam, which, when targeted at a small blunt object, can generate a hypersonic shock layer that exhibits highly relevant shock layer chemistry. Initial experimental studies of Kapton H ablation by a hypersonic O/O_2 beam in conjunction with DSMC calculations confirm the presence of a shock layer above a 25 mm dia. test object. This shock layer, while rarefied, is a repeatable nonequilibrium environment that may be exploited for hypersonics research and testing. While the initial tests are promising, further enhancements are envisioned that would produce higher densities in the shock layer. In addition, beams with various mole fractions of O, O_2, N, N_2, and NO are envisioned. Thus, the TTST represents an approach to materials testing and studies of nonequilibrium chemistry in a hypersonic flow environment that can be produced in a laboratory-scale instrument. Unlike large shock-tunnel facilities, the beam, and therefore the shock layer, can be generated (pulsed) 2-3 times per second for hours or even days with repeatable conditions. Such test frequency and repeatability will enable existing optical and mass spectrometric diagnostic techniques to measure thermochemical quantities in realistic nonequilibrium chemistry conditions with unprecedented accuracy and precision at a small fraction of the cost compared to existing shock tunnel facilities. The new capability can also provide rapid screening for

emerging materials and allow informed selection of materials for more expensive tests in high-enthalpy test facilities. Results obtained so far indicate that the TTST is a promising new and complementary tool in the hypersonics community that can produce data for nonequilibrium dissociation, vibrational and rotational populations, gas-surface interactions, and material response phenomena.

Acknowledgments

This work was supported by the US Air Force Office of Scientific Research (Grant Number FA9550-19-1-01120 and by the US Air Force Research Lab (Grant Numbers FA9453-20-1-0052 and FA9453-20-1-0012). The views expressed herein are those of the authors and do not necessarily represent the official policies or endorsements, either expressed or implied, of the AFOSR, AFRL, or the US government.

References

[1] Leyva, I. A. The Relentless Pursuit of Hypersonic Flight. *Physics Today* **2017**, *70*, 30-35.

[2] Millikan, R. C.; White, D. R. Systematics of Vibrational Relaxation. *J. Comp. Phys.* **1953**, *39*, 3209-3213.

[3] Park, C. *Nonequilibrium Hypersonic Aerothermodynamics* (Wiley, New York, 1990).

[4] Paukku, Y.; Yang, K. R.; Varga, Z.; Truhlar, D. G. Global Ab Initio Ground State Potential Energy Surface of N_4. *J. Chem. Phys.* **2013**, *139*, 044309.

[5] Bender, J. D.; Valentini, P.; Nompelis, I.; Paukku, Y.; Varga, Z.; Truhlar, D. G.; Schwartzentruber, T. E.; Candler, G. V. An Improved Potential Energy Surface and Multi-Temperature Quasiclassical Trajectory Calculations of N_2 + N_2 Dissociation Reactions. *J. Chem. Phys.* **2015**, *143*, 054304.

[6] Valentini, P.; Schwartzentruber, T. E.; Bender, J. D.; Candler, G. V. Dynamics of Nitrogen Dissociation from Direct Molecular Simulation. *Phys. Rev. Fluids* **2016**, *1*, 043402.

[7] Valentini, P.; Schwartzentruber, T. E.; Bender, J. D.; Nompelis, I.; Candler, G. V. Direct Molecular Simulation of Nitrogen Dissociation Based on an Ab Initio Potential Energy Surface. *Phys. Fluids* **2015**, *27*, 086102.

[8] Panesi, M.; Jaffe, R. L.; Schwenke, D. W.; Magin, T. E. Rovibrational Internal Energy Transfer and Dissociation of N_2-N System in Hypersonic Flows. *J. Chem. Phys.* **2013**, *138*, 044312.

[9] Kim, J. G.; Boyd, I. D. State-Resolved Master Equation Analysis of Thermochemical Nonequilibrium of Nitrogen. *Chem. Phys.* **2013**, *415*, 237–246.

[10] Byron, S. Shock-Tube Measurement of the Rate of Dissociation of Nitrogen. *J. Chem. Phys.* **1966**, *44*, 1378.

[11] Appleton, P.; Steinberg, M.; Liquornik, D. J. Shock-Tube Study of Nitrogen Dissociation using Vacuum-Ultraviolet Light Adsorption. *J. Chem. Phys.* **1968**, *48*, 599; erratum: **1968**, *49*, 2468.

[12] Hanson, K.; Baganoff, D. Shock-Tube Study of Nitrogen Dissociation Rates Using Pressure Measurements. *AIAA J.* **1972**, *10*, 211.

[13] Holden, M. S.; MacLean, M.; Wadhams, T. P.; Dufrene, A. Measurements of Real Gas Effects on Regions of Laminar Shock Wave/Boundary Layer Interaction in Hypervelocity Flows for 'Blind' Code Validation Studies. Presented at the *21st AIAA Computational Fluid Dynamics Conference*, June 24-27, 2013, San Diego, CA; Paper No. AIAA 2013-2837.

[14] Lewis, S. W.; Morgan, R. G.; McIntyre, T. J.; Alba, C. R.; Greendyke, R. B., Expansion Tunnel Experiments of Earth Reentry Flow with Surface Ablation. *J. Spacecr. Rockets* **2016**, 53, 887-899.

[15] Cruden, B. A.; Prabhu, D.; Martinez, R.; Lee, H.; Bose, D.; Grinstead, J. H. Absolute Radiation Measurements in Venus and Mars Entry Conditions. AIAA Paper 2010-4508.

[16] Krishna, Y.; Sheehe, S. L.; O'Byrne, S. B. A Time-Resolved Temperature Measurement System for Free-Piston Shock Tunnels. *31st AIAA Aerodynamic Measurement Technology and Ground Testing Conference, AIAA Aviation*, Paper No. AIAA 2015-2249.

[17] Swantek, A. B.; Austin, J. M. Flowfield Establishment in Hypervelocity Shock-Wave/Boundary-Layer Interactions. *AIAA J.* **2015**, *53*, 311-320.

[18] Winters, C.; Chernukho, A.; Eckert, Z.; Adamovich, I. V. Measurements and Kinetic Modeling of OH and H Number Densities in Nanosecond Pulse Discharges in C_xH_y-O_2-Ar and C_xH_y-Air Mixtures. *54th AIAA Aerospace Sciences Meeting, AIAA SciTech*, Paper No. AIAA 2016-1211.

[19] Caledonia, G. E.; Krech, R. H.; Green, B. D. A High-Flux Source of Energetic Oxygen-Atoms for Material Degradation Studies. *AIAA J.* **1987**, *25*, 59-63.

[20] Zhang, J.; Garton, D. J.; Minton, T. K. Reactive and Inelastic Scattering Dynamics of Hyperthermal Oxygen Atoms on a Saturated Hydrocarbon Surface. *J. Chem. Phys.* **2002**, *117*, 6239-6251.

[22] Garton, D. J.; Brunsvold, A. L.; Minton, T. K.; Troya, D.; Maiti, B.; Schatz, G. C. Experimental and Theoretical Investigations of the Inelastic and Reactive Scattering Dynamics of $O(^3P)$ + D_2. *J. Phys. Chem. A* **2006**, *110*, 1327-1341.

[23] Minton, T. K.; Schwartzentruber, T. E.; Xu, C. On the Utility of Coated POSS-Polyimides for Vehicles in Very Low Earth Orbit. *ACS Appl. Mater. Interfaces* **2021**, *13*, 51673-51684.

[24] Garton, D. J.; Minton, T. K.; Maiti, B.; Troya, D.; Schatz, G. C. A Crossed Molecular Beams Study of the $O(^3P)+H_2$ Reaction: Comparison of Excitation Function with Accurate Quantum Reactive Scattering Calculations. J. Chem. Phys. 2003, 118, 1585−1588.

[25] Troya, D.; Schatz, G. C.; Garton, D. J.; Brunsvold, A. L.; Minton, T. K. Crossed Beams and Theoretical Studies of the $O(^3P)+CH_4 \rightarrow H+OCH_3$ Reaction Excitation Function. *J. Chem. Phys.* 2004, *120*, 731.

[26] Silverman, E. M. Space Environmental Effects on Spacecraft: LEO Materials Selection Guide. NASA CR 4661, Part 1, August 1995.

[27] Buczala, D. M.; Brunsvold, A. L.; Minton, T. K. Erosion of Kapton H by Hyperthermal Atomic Oxygen. *J. Spacecraft and Rockets* **2006**, *43*, 421-425.

[28] de Groh, K. K.; Banks, B. A. MISSE PEACE Polymers Erosion Morphology Studies. *Proceedings of the International Symposium on Materials in a Space Environment (ISMSE-11)*, September 15-18, 2009, Aix-en-Provence, France, 2009.

[29] Bird, G. Direct Simulation and the Boltzmann Equation. *The Physics of Fluids*, Vol. 13, No. 11, 1970, pp. 2676–2681.